DENSIFICATION AND EFFECT OF COMPRESSION RATIO ON MECHANICAL PROPERTIES OF CLT FROM LOW-DENSITY TIMBER

KANG CHIANG LIEW, YU FENG TAN
UNIVERSITI MALAYSIA SABAH
MALAYSIA

ABSTRACT

The mechanical properties of CLT manufactured from densified low-density planted timber, *Paraserianthes falcataria* were studied in relation to changes in the area of pores for under densification. Conditioned laminas (MC $\leq$ 15%) underwent two-stage densification using hot-press machine at 105°C, 6 MPa, for 10 min each, with press released for 1 min 40 sec in between the stages, before cooling ($< 100^{\circ}$C) to reduce immediate springback. The laminas with thickness 8 mm, 10 mm, and 15 mm were produced using metal stoppers and further manufactured into three-layered CLT of 24 mm, 30 mm, and 45 mm thick. 20 mm undensified laminas with 60 mm CLT as the control. Results shows that modulus of elasticity (MOE), modulus of rupture (MOR), and compression parallel to grain have improved significantly and showed negative correlation with area of pores, except for compression perpendicular to grain.

KEYWORDS: Wood densification, low-density planted timber, cross-laminated timber, mechanical properties, morphology.

INTRODUCTION

The increasing in illegal and unplanned logging activities is pushing the depletion of these naturally grown resources. Therefore, initiatives such as promoting the use of fast-growing plantation wood species were implemented to cope with the challenges of timber. The inherent property of wood materials from planted forests was their lower density when compared to naturally grown wood (Hashim et al. 2015). Due to its fast-growing ability and short harvest rotation, the trunks tend to have smaller diameters with limited strength.

One of the emerging modification technologies targeting the improvement of density is densification. Densification process is carried out by compressing the wooden board between heated metal plates under suitable temperature, time, and pressure. During this process,

_____

the thickness of the wooden board tends to reduce due to the reduction of void spaces in the fibers' lumen and is fixed under a compressed state, hence increasing the overall density of wood (Laine et al. 2016). The softened/plasticized cell wall polymer under certain heating periods allows the structures to be compressed and permits a certain degree of change in thickness. These changes in thickness are known as the compression ratio, and they are proportional to the density of wood (Kutnar et al. 2008, Pelit et al. 2014, Bao et al. 2017).

The thin-walled, low-density plantation wood provides greater potential to be transformed into a higher density product through the densification process. However, the major drawback associated with the densification of wood is the spingback effect. The springback effect is the tendency of wood material to revert to its original dimension after densification when the pressure applied to it is removed (Neyses 2016). Such a phenomenon would affect the final density and properties of wood materials.

As there is limited literature on the potential of densified wood to be constructed into engineered wood products, such an attempt could generate important information for the future development of the wood-based industry. In this study, low-density plantation wood, *P. falcataria*, was densified under simple equipment, which is the hot-press machine, to different targeted thicknesses. The densified laminas were then used to construct engineered wood products with a cross-laminated timber (CLT) arrangement to reduce springback effects. The cross-orientation arrangement of CLT is known to provide better stability (Harris 2015). The mechanical properties of CLT and their relationship with the morphology of densified *P. falcataria* were investigated.

MATERIAL AND METHODS

Materials

Fast-growing tropical plantation timber *P. falcataria* with density in the range of $220 - 430$ $kg \cdot m^{-3}$ were used in this study. The timber was supplied by Sapulut Forest Development Sdn. Bhd. in the form of sawn laminas with dimensions of 300 mm (L) x 50 mm (W) x 20 mm (T). The sawn, planned, and kiln-dried laminas were left to condition at relative humidity of 65%, $20^{o}C$ until the average moisture content reaches 12% - 15%. Laminas with big knots and visible irregularities were visually graded and excluded as it could be affected during densification process.

Densification method

The densification methods in this study were adapted from Kutnar et al. (2011) and Pelit et al. (2016). A two-stage densification was carried out using a specially designed hot-press machine equipped with water cooling system. First, laminas were densified in between the heated platens at temperature of $105^{o}C$ with 6 MPa compressing at the radial direction of laminas for 10 min. After that, the press was released (venting) for 1 min 40 sec to induced mechano-sorption effect by releasing some moisture trapped in the cell structures of laminas. Second stage of densification was then carried out again at $105^{o}C$, 6 MPa, for 10 min. Finally, the heat was turned off and water-cooling system was activated while the laminas were still pressed for the laminas to

_____

cool down until temperature of approximately 80ºC to reduce immediate springback. During the pressing operation, special metal stoppers with thicknesses of 8 mm, 10 mm, and 15 mm were utilized which resulted in three different compression ratios (CR) of 60%, 50%, respectively according to Eq. 1 (Laine et al. 2016). Undensified laminas (20 mm) were used as control:

$$Compression\ ratio\ (\%): \frac{T_o - T1}{T_o} \times 100\% \tag{1}$$

where: T_o - original thickness (mm) of laminas, $T1$ - targeted thickness (mm) after densification.

Area of pores determination

Morphological examination was done to determine the changes in area of pores for laminas under densification at different targeted thicknesses. Small test pieces with size of 5 mm (L) x 5 mm (W) x 5 mm (T) each from densified (8 mm, 10 mm, and 15 mm) and undensified (20 mm) laminas were cut out for Scanning electron microscopy (SEM) examination. SEM images were used to determine the area of pores for densified and undensified laminas through ImageJ software.

Cross-laminated timber (CLT) manufacturing process

The densified and undensified laminas were finger-cutted and joined into 1 meter long strips using PVAc glue to obtain finger jointed CLT panel according to BS EN 16351. PVAc was commonly used in the wood-based industries for gluing wood components. The strips were then cut into 300 mm length and were further edge and face glued to produce three layered CLT of size 300 mm (L) x 300 mm (W) with different total thickness (T) of 24 mm, 30 mm, 45 mm, and 60 mm due to the varying thickness of laminas (8 mm, 10 mm, 15 mm, and 20 mm). Coding of CLT 24, CLT 30, CLT 45, and CLT 60 were used to differentiate the CLT test pieces as shown in Tab. 1.

Tab. 1: Coding of three-layered CLT manufactured from different thicknesses of laminas with different compression ratio.

Coding	Compression ratio (%)	Thickness of laminas (mm)	Thickness of three-layered CLT (mm)
CLT 24	60	8	24
CLT 30	50	10	30
CLT 45	25	15	45
CLT 60	0	20	60

It is important to note that the middle layer of the three-layered CLT was oriented 90º to the subsequent layers to form longitudinal-tangential-longitudinal (LTL) arrangement as shown in Fig. 1.
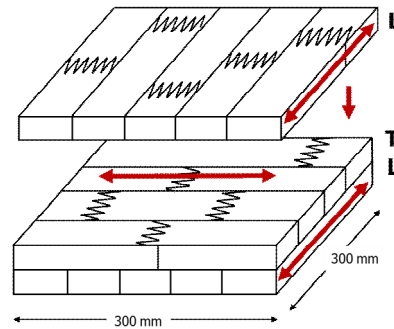
Fig. 1: Longitudinal-tangential-longitudinal (LTL) arrangement of three-layered CLT.

Bending properties (flatwise versus edgewise tests)

Bending strength test was carried out using Universal Testing Machine (UTM) according to ASTM D198-05a (2008). The dimension of the test piece was 300 mm (L) x 50 mm (W) x (24, 30, 45, 60) mm (T) with span length (L) set at 264 mm before locating the test piece symmetrically on the supports. Center-point loading test setup was employed due to the smaller scale of test piece, with testing speed of 3 mm·min^{-1} for the maximum load (P) to be achieved within 6 – 20 min.

Two different positions for bending test were carried out according to BS EN 16351 (2015), where maximum load (P) was recorded for modulus of elasticity (MOE) and modulus of rupture (MOR) and later calculated based on Eqs. 2 and 3. The positions were flatwise (loads perpendicular to the plane) (Fig. 2a) and edgewise (loads in plane direction) (Fig. 2b) to compare the effects of CLT panels for better understanding of CLT in application. 30 test pieces were prepared for each position.

$$MOE \ (N/mm^2) = \frac{PL^3}{4bd^3\Delta} \tag{2}$$

$$MOR \ (N/mm^2) = \frac{3PL}{2bd^2} \tag{3}$$

where: *P*- load below proportional limit (N), *L*- distance between supports/span (mm), *b* - width of test piece (mm), *d* - thickness of test piece/depth (mm), *Δ* - direction in corresponding to load *P* (mm).
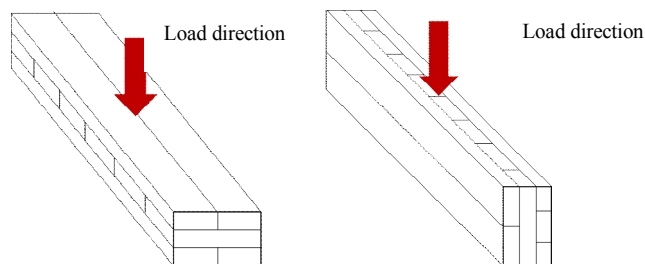
Fig. 2: Bending strength testing with load applied, (a) perpendicular to the grain (flatwise testing), (b) in plane direction (edgewise testing).

_____

Compression strength (parallel versus perpendicular to the grain)

30 test pieces with size of 200 mm (L) x 50 mm (W) x (24, 30, 45, 60) mm (T) were obtained from CLT panels according to ASTM D143-94 (2008). Compressive load was applied in axial direction (compression parallel to the grain) (Fig. 3a) until failures occurred. After several preliminary tests, the test speed was set at 1 mm·min^{-1} so that maximum load force was reached within 5 min as stipulated in BS EN 408 (2010).

For compression perpendicular to the grain, 30 test pieces of 150 mm (L) x 50 mm (W) x (24, 30, 45, 60) mm (T) were prepared based on ASTM D143-94 (2007). Compressive load was applied perpendicularly to the axis of test piece (Fig. 3b). After that, constant test speed of 5 mm·min^{-1} was applied for maximum force to reach within 5 min until failure was detected (BS EN 408, 2010). Compression strength for parallel and perpendicular to the grain were calculated using Eq. 4.
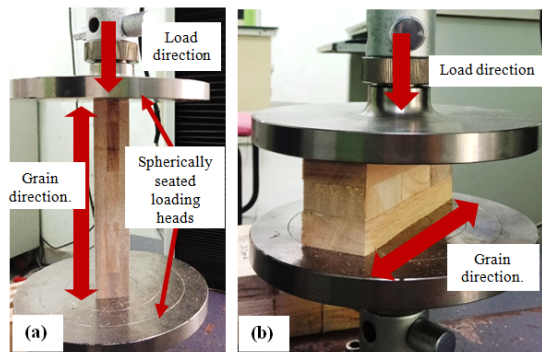
Fig. 3: Positioning of the test piece for compression, a) parallel to the grain direction, b) perpendicular to the grain direction.

$$Compressive\ strength\ (N/mm^2) = \frac{Fmax}{A} \tag{4}$$

where: *Fmax* - maximum load applied (N), *A* - area of test piece (mm^2).

RESULTS AND DISCUSSION

Area of pores determination

Fig. 4 depicts the raw data dispersion of area of pores at different targeted thickness of laminas. It shows that 20 mm undensified laminas (control) has wider dispersion for area of pores values. This is due to the naturally occurred variable sizes/area of pores in the laminas. Overall, the trend shows that the compression ratio of densification is inversely proportional to the size of pores. This is similar to the findings by Bekhta et al. (2016). Besides, Tan and Liew (2021) reported that, statistically significant (p ≤ 0.05) were detected when comparing densified laminas at different thicknesses to the undensified laminas. The increase in density can be observed with the loss of porosity. Figs. 5a–d illustrates the SEM micrographs for area of pores in different targeted thickness of densified and undensified laminas at 800X magnification.
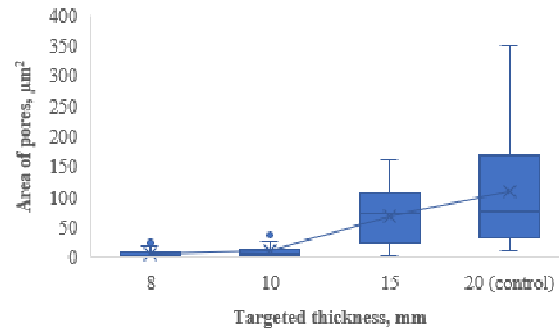
Fig. 4: Box and whisker plots indicate median, 25% and 75% percentile, maximum and minimum (bars) for area of pores in laminas densified at different targeted thickness (8 mm, 10 mm, and 15 mm) with undensified laminas (20 mm) as control.
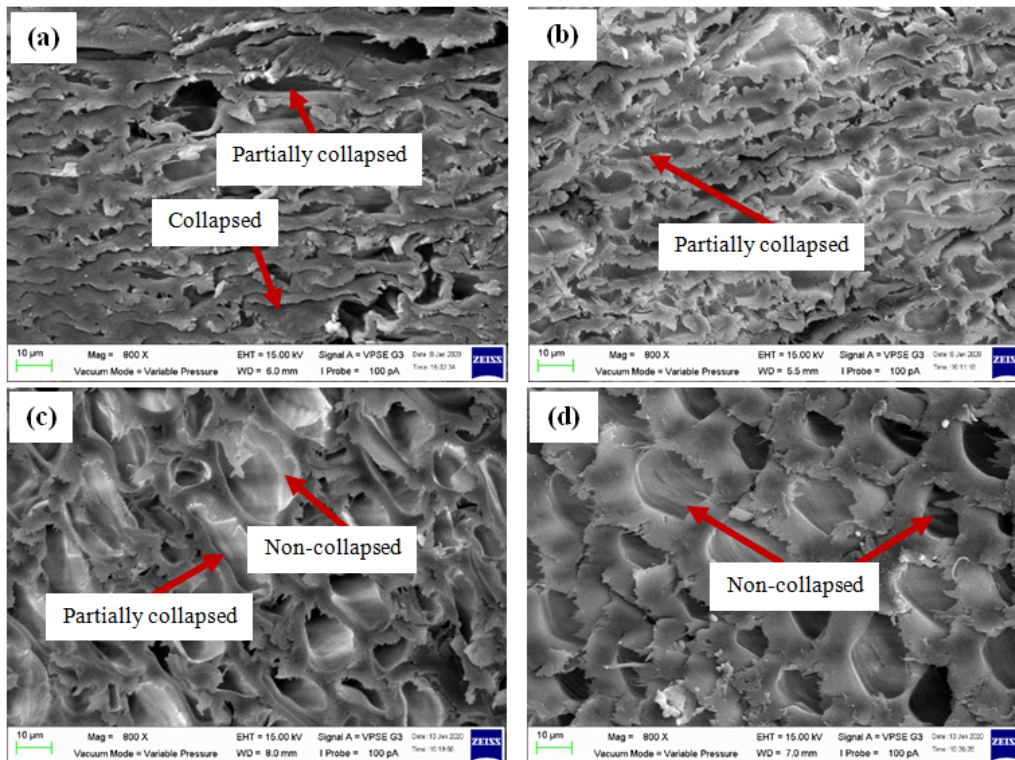
Fig. 5: SEM micrographs for area of pores in, (a) 8 mm targeted thickness with collapsed and partially collapsed pores (arrows), (b) 10 mm targeted thickness with mostly partially collapsed pores, (c) 15 mm targeted thickness with partially and non-collapsed pores at surface of laminas, (d) 20 mm undensified laminas with non-collapsed pores.

Bending properties (flatwise versus edgewise tests) of CLT and its correlation with area of pores.

Tab. 2 depicts the results for modulus of elasticity (MOE), modulus of rupture (MOR) at flatwise and edgewise bending test, compression strength test at parallel and perpendicular to the grain direction for CLT manufactured from different thickness of densified and undensified laminas. The highest MOE recorded was 2968.1 N·mm^{-2}, while 32.2 N·mm^{-2} was for MOR. These values were obtained from CLT 24 (8 mm densified laminas) positioned at edgewise

_____

direction (Tab. 2). These results were compared with findings by Tan and Liew (2021) on MOE and MOR tested in flatwise direction as shown in Fig. 6.

Tab. 2: Statistical analysis (mean and standard deviations) for bending properties of three-layered CLT manufactured from densified and undensified laminas (Tan and Liew 2021).

Compression ratio of laminas (at different thickness) (%)	Total thickness of three-layered CLT (mm)	Bending properties			
		Flatwise*		Edgewise	
		MOE (N·mm⁻²)	MOR (N·mm⁻²)	MOE (N·mm⁻²)	MOR (N·mm⁻²)
60	24	2348.1 (108.7)a	26.7 (5.2)a$^{\#}$	2968.1 (585.9)a$^{\#}$	32.2 (6.0)a
50	30	1348.1 (161.3)b	21.3 (5.0)b$^{\#}$	2439.9 (362.1)b$^{\#}$	31.9 (8.2)a
25	45	558.7 (115.1)c	16.0 (2.4)c	1726.7 (180.5)c	20.7 (6.0)b$^{\#}$
0	60	294.9 (22.9)d$^{\#}$	13.7 (0.9)d$^{\#}$	1290.7 (75.1)d$^{\#}$	21.92 (3.8)b

Note: Different alphabets (a, b, c, and d) within a column of different targeted thicknesses for each test indicates significant difference at $p \leq 0.05$. $^{\#}$ Refer to the existence of non-zero correlation.

(a) Thickness of CLT, mm

■ MOE (Flatwise) ■ MOE (Edgewise)

(b) Thickness of CLT, mm

■ MOR (Flatwise) ■ MOR (Edgewise)
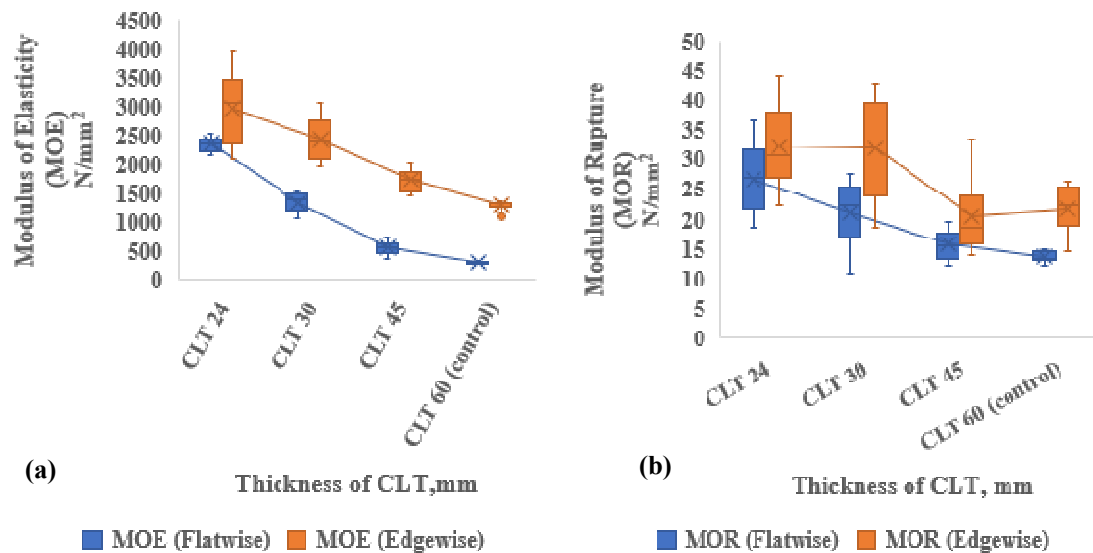
Fig. 6: Box and whisker plots indicate median, 25% and 75% percentile, maximum and minimum (bars) for, (a) modulus of elasticity (MOE) according to different thickness of densified CLT (CLT 24, CLT 30, and CLT 45) and undensified/control (CLT 60) at flatwise and edgewise testing, (b) modulus of rupture (MOR) according to different thicknesses of densified CLT (CLT 24, CLT 30, and CLT 45) and undensified/control (CLT 60) at flatwise and edgewise testing.

Graphs of MOE and MOR (flatwise vs. edgewise) were obtained from 30 replicates each for each CLT coding. From Fig. 6a, CLT of densified laminas positioned edgewise shows higher overall MOE value as compared to flatwise. Statistically significant ($p \leq 0.05$) can be seen among different thicknesses of CLT at flatwise (MOE and MOR) and edgewise (MOE) (Tab. 2). MOE and MOR of CLT 24 at edgewise bending test have improved significantly by 129.96% and 46.85%, respectively. Increase in MOE and MOR for bending at edgewise were lower as compared to the improvement of MOE and MOR in flatwise bending in which the percentage increase recorded were 696.11% and 95.46%, respectively. Laminas densified into 15 mm,

_____

10 mm, and 8 mm, which have CR of 25%, 50%, and 60%, respectively leads to higher density and hence, improves the bending properties of laminas. Such finding corresponded to Kutnar et al. (2008) and Bao et al. (2017).

The lower MOR of CLT 60 (control) at both flatwise and edgewise might be due to the large volume of wood which have higher critical strength-reducing defects that led to lower value in the bending test. Besides, there is slightly odd with the trend of CLT's MOR positioned edgewise at which the CLT manufactured from 15 mm thick densified laminas has lower boxplot (average value of 20.68 N$\cdot$mm^{-2}) as compared to control (20 mm thick laminas) which has average of 21.9 N$\cdot$mm^{-2}. Inconsistent SB effect of 15 mm surface-densified laminas with lower core density might have attributed to this. Such outcomes also proven by Sikora et al. (2016) and Li (2017).

The findings of this study (higher MOE and MOR tested in edgewise direction) might be due to the 90° orientation of laminations in CLT at which stresses are distributed equally among each layer of laminas and acted together as one body in sustaining the load imparted upon it when tested at edgewise. In a flatwise test, the bottom layer of CLT, which usually consists of one or two pieces of laminas joined by finger joints, were subjected to maximum forces until ruptured. This is evident by the failure modes of CLT tested in flatwise direction mostly taking place between bottom and middle layer. The findings in this study reveals the opposite as compared to Bal and Bektaş (2012) and Bal (2016) and this is due to the difference in product tested as these authors' work were based on laminated veneer lumber (LVL).

However, it is important to note that for MOR in edgewise position, no statistically significant (p > 0.05) were detected between CLT 24 and CLT 30, as well as between CLT 45 and CLT 60 (Tab. 2). Such differences may be due to porosity differences, as CLT 24 and CLT 30 made from 8 mm and 10 mm densified laminas, respectively, have more collapsed and partially collapsed pores, as shown in area of pores determination section. CLT 45, on the other hand, was made of 15 mm densified laminas and has more non-collapsed pores, with the only pores at the surface of the laminas partially collapsed. The availability of non-collapsed pores present in CLT 45 might have contributed to the no significant difference of MOR result as compared to CLT 60. The more compact cell structures (higher density) eventually provide higher ability for the CLT to withstand stresses imparted to prevent the potential bending failures. In other words, stresses could be distributed more rapidly across cell structures.

Correlation analyses were further carried out to determine the effect of changes in area of pores due to densification process on the MOE and MOR of CLT. The reduction in area of pores (from 20 mm to 8 mm) laminas showed significantly high negative correlation (r = -0.526) to MOE of CLT while MOR shows medium negative correlation (r = -0.356) in edgewise bending. The same negative correlation trend was reported in Tan and Liew (2021) for MOE and MOR of flatwise bending. Fig. 7a and b portrays the correlation between area of pores at different thicknesses of laminas with MOE and MOR at edgewise of CLT.
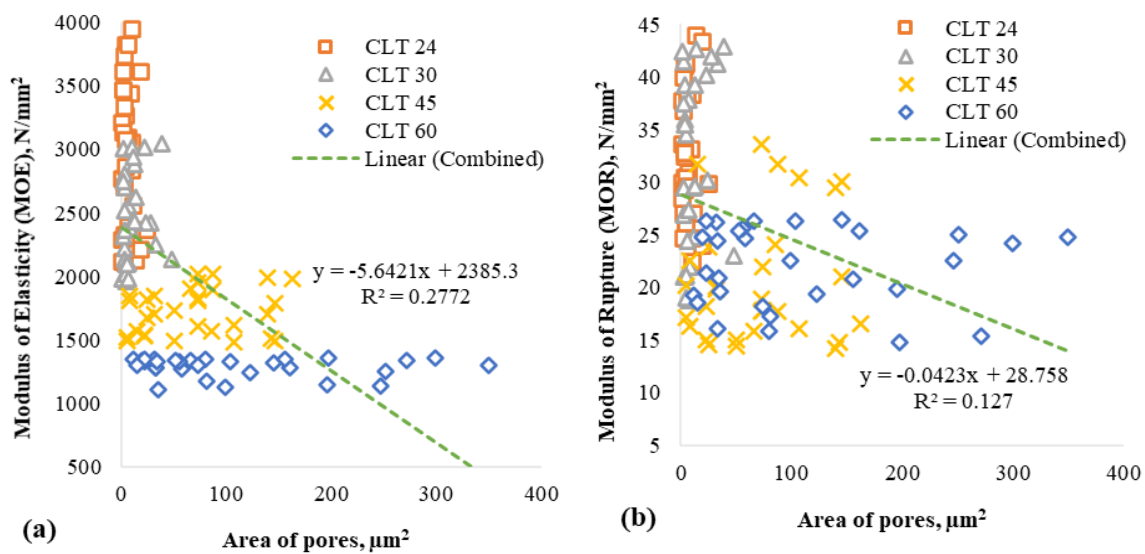
Fig. 7: Correlation between morphology (area of pores) of densified and undensified laminas, (a) modulus of elasticity (MOE) of CLT panels manufactured from the laminas positioned at edgewise direction, (b) modulus of rupture (MOR) of CLT panels manufactured from the laminas positioned at edgewise direction.

The R^2 values in both graphs showed that the MOE and MOR have weak interactions with the area of pores. This is because not all parameters (CLT 24, CLT 30, CLT 45, and CLT 60) correlate with the area of pores when analyzed individually as shown in Tab. 2. Overall, bending properties of CLT increases with decreasing area of pores in laminas. This is expected as the softening of lignin and hemicellulose permits the fibers to be compressed and become denser thus improving bending properties. It is important to note that the softening of hemicelluloses and lignin took place at $54 - 56^{o}C$ and $72-128^{o}C$, respectively (Kutnar and Šernek 2008, Kutnar et al. 2009, Tu et al. 2014, Rautkari et al. 2011). Shi et al. (2020) found a similar trend of correlation in densified wood combined with chemical pre-treatment. Remarkably, densification temperature of $105^{o}C$ did not cause severe degradation of hemicelluloses and lignin which then contributes to the higher MOE and MOR of CLT. Cellulose, hemicelluloses, and lignin as well as the chain and crosslinked microfibrils are the factors contributed to the mechanical properties of laminas (Wagner et al. 2015).

Compression strength (parallel versus perpendicular to the grain) and its correlation with area of pores.

Tab. 3 provides the average values of compressive strength for both parallel and perpendicular to the grain. No statistically significant ($p > 0.05$) was found between CLT 24 and CLT 30 with the average value recorded at 18 $N{\cdot}mm^{-2}$ and 17.4 $N{\cdot}mm^{-2}$ as shown in Tab. 3. Furthermore, statistically significant ($p \leq 0.05$) is detected for CLT 45 and CLT 60 as compared within groups for compressive strength at parallel to the grain. This phenomenon might be due to the CR of densified laminas at which the CR 25% and above has a significant effect on the CLT panel manufactured. Laminas subjected to higher CR during densification process resulted in

_____

higher compression strength parallel to grain with the increase in density of laminas. Fig. 8 illustrated the trend of CLT at parallel and perpendicular to the grain direction. CLT at parallel to grain direction shows a trend in which the compressive strength increases with descending order of CLT thickness. This is in line with the findings of Pelit et al. (2018).

Tab. 3: Statistical analysis (mean and standard deviations) for bending properties of three-layered CLT manufactured from densified and undensified laminas.

Compression ratio of laminas (at different thickness) (%)	Total thickness of three-layered CLT (mm)	Compression strength	
		Parallel (N$\cdot$mm^{-2})	Perpendicular (N$\cdot$mm^{-2})
60	24	18.0 (2.9)a[#]	13.1 (0.9)a
50	30	17.4 (1.8)a[#]	13.4 (1.5)ab
25	45	13.5 (2.8)b	13.1 (0.6)a
0	60	11.5 (0.8)c	13.9 (0.6)b[#]

Note: Different alphabets (a, b, c, and d) within a column of different targeted thicknesses for each test indicates significant difference at p ≤ 0.05. [#] Refer to the existence of non-zero correlation.
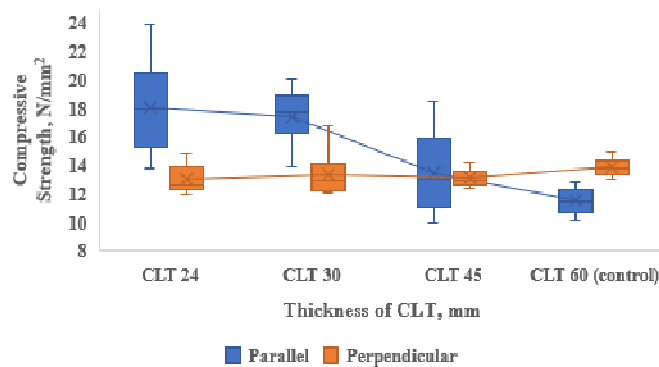
Fig. 8: Box and whisker plots indicate median, 25% and 75% percentile, maximum and minimum (bars) for compressive strength according to different thickness of densified CLT (CLT 24, CLT 30, and CLT 45) and undensified/control (CLT 60) at parallel and perpendicular to the grain testing.

CLT 24, CLT 30, and CLT 45 with average value of 13.1 N$\cdot$mm^{-2}, 13.4 N$\cdot$mm^{-2}, and 13.1 N$\cdot$mm^{-2}, respectively, did not show significant effect (p > 0.05) among each other when load was applied perpendicular to the grain direction as shown in Tab. 3. This suggests that increasing the CR has no influence on the compression strength of CLT tested perpendicular to the grain direction. Such phenomenon might be due to the compression perpendicular to the grain tends to compress the fibers in the radial direction, which was similar to the densification process in this study. The porous structures of CLT 60 (control) made from undensified (20 mm) laminas have more void spaces that can be squeezed, resulting in higher compressive strength perpendicular to grain. CLT made from densified laminas, on the other hand, had been compressed during the densification process. As the cell lumens had collapsed during densification process, the excessive deformation of CLT during compression strength test at perpendicular to the grain direction were minimalised. Therefore, only the comparison with CLT 60 (undensified/control) was statistically significant (p ≤ 0.05).

_____

Besides, higher contact areas between the load and the surface of the CLT might result in decreased strength. In the case of this study, the areas of all the CLT test pieces for compression perpendicular to the grain test were constant. Therefore, no obvious fluctuation was observed in Fig. 8. However, for compression strength parallel to grain, the load bearing area of CLT was different due to the different thicknesses of laminas (8 mm, 10 mm, 15 mm, and 20 mm) used. This explains the trend in which higher compression strength parallel to grain was observed in CLT 24 (smaller contact areas). This finding agrees well with the theory of Brandner (2018).

Figs. 9a,b illustrate the correlation between area of pores from different thicknesses of laminas (densified and undensified) and compressive strength of CLT parallel to grain. The overall (N = 120) trend shows that area of pores (from 8 mm to 20 mm) has significant negative medium correlation (r = -0.488) with compression strength parallel to grain of CLT (Fig. 9a). The R^2 values in both graphs also showed weak interactions between compression strength and area of pores in both tested directions. This is because not all parameters (CLT 24, CLT 30, CLT 45, and CLT 60) have correlation with the area of pores when analyzed individually as shown in Tab. 3. Indeed, the occurrence of more deformed cell (collapses, breakage, cracks, etc.) under high CR of densification might reduce the strength properties as confirmed by other studies (Kutnar et al. 2009, Budakçı et al. 2016, Bekhta et al. 2017, Pelit and Yorulmaz 2019).
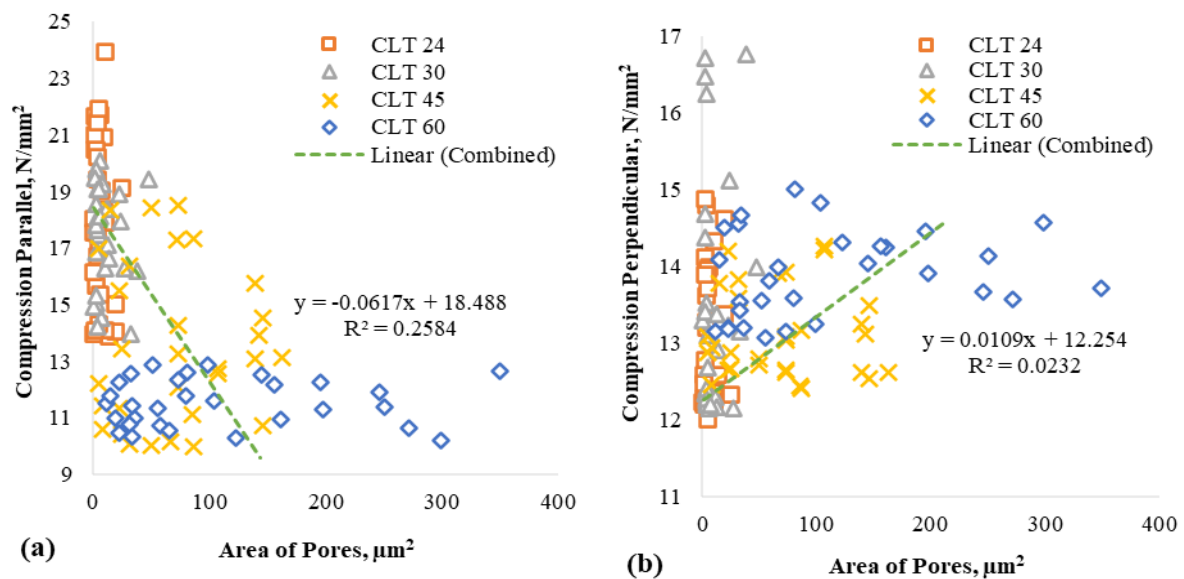
Fig. 9: Correlation between morphology (area of pores) of densified and undensified laminas with compression strength of CLT panels manufactured from the laminas positioned, (a) parallel to the grain direction, (b) perpendicular to the grain direction.

Apart from that, Fig. 9b presented the area of pores for laminas at different thicknesses (densified and undensified) and the compressive strength of CLT perpendicular to the grain. Only undensified (control) area of pores of laminas has weak positive correlation (r = 0.210) with CLT's compressive strength perpendicular to grain. Area of pores for densified laminas shows no correlations with compressive strength perpendicular to grain of CLT. As discussed earlier,

_____

such phenomenon might be due to the availability of compressible pores are limited as most pores in densified laminas were already collapsed. Serrano and Enquist (2010) revealed that when loaded perpendicular to the grain, the compressive strength of CLT was significantly dependent on the loading scenario such as uniform pressure/line load, loading close to edge, line load parallel or perpendicular to surface layer grain direction.

CONCLUSIONS

The results obtained show that mechanical properties such as bending and compression parallel to the grain properties of CLT manufactured from laminas which undergone densification process have improved with the decreasing in thickness. The decreasing in thickness of laminas accompanied by densification process had successfully reduced the area of pores with no fractures to the cell walls. Such phenomenon has contributed to the improvement in strength properties. Edgewise bending test has improved significantly by 129.96% (MOE) and 46.85% (MOR) compared to CLT 60 (undensified). Compression parallel to grain increases significantly to 18.03% (CLT 24), but compression perpendicular to grain shows no significant difference among CLT of densified laminas. Besides, the reduction in area of pores had showed strong negative correlation with MOE flatwise and edgewise bending. Meanwhile, MOR of flatwise and edgewise bending, and compression parallel to the grain have medium negative correlation. Only compression perpendicular to the grain was proportional area of pores.

ACKNOWLEDGMENTS

REFERENCES

1. ASTM D 143-94, 2008: Standard test methods for small clear specimens of timber.
2. ASTM D 198-05a, 2008: Standard test methods of static tests of lumber in structural sizes.
3. Bal, B.C., Bektaş, I, 2012: The effects of wood species, load direction, and adhesives on bending properties of laminated veneer lumber. BioResources 7(3): 3104-3112.
4. Bal, B.C., 2016: Some technological properties of laminated veneer lumber produced with fast-growing poplar and eucalyptus. Maderas. Ciencia y Tecnologia 18(3): 413-424.
5. Bao, M., Huang, X., Jiang, M., Yu, W., Yu, Y., 2017: Effect of thermo-hydro-mechanical densification on microstructure and properties of poplar wood (*Populus tomentosa)*. Journal of Wood Science 63(6): 591-605.
6. Bekhta, P., Mamoňová, M., Sedliačik, J., Novák, I., 2016: Anatomical study of short-term thermo-mechanically densified alder wood veneer with low moisture content. European Journal of Wood and Wood Products 74(5): 643-652.
7. Bekhta, P., Proszyk, S., Krystofiak, T., Sedliacik, J., Novak, I., Mamonova, M., 2017: Effects of short-term thermomechanical densification on the structure and properties of wood veneers. Wood Material Science & Engineering 12(1): 40-54.

8. BS EN 408, 2010: Timber structures. Structural timber and glued laminated timber. Determination of some physical and mechanical properties.

9. BS EN 16351, 2015: Timber structures. Cross laminated timber. Requirements.

10. Brandner, R., 2018: Cross laminated timber (CLT) in compression perpendicular to plane: testing, properties, design and recommendations for harmonizing design provisions for structural timber products. Engineering Structures 171: 944-960.

11. Budakçı, M., Pelit, H., Sönmez, A., Korkmaz, M., 2016: The effects of densification and heat post-treatment on hardness and morphological properties of wood material. BioResources 11(3): 7822-7838.

12. Harris, R., 2015: Cross laminated timber. In: Wood composites (ed. Ansell MP). Pp 141-167, Woodhead Publishing. United Kingdom.

13. Hashim, M.N., Mohd Hazim, M.A., Syafinie, A.M., 2015: Strategic forest plantation establishment in Malaysia for future product development and utilization. Proceedings of Kuala Lumpur International Agriculture, Forestry and Plantation. Malaysia. Pp 14 - 24.

14. Kutnar, A., Šernek, M., 2008: Densification of wood. Zbornik gozdarstva in lesarstva 82: 53-62.

15. Kutnar, A., Kamke, F.A., Sernek, M., 2008: The mechanical properties of densified VTC wood relevant for structural composites. Holz Roh Werkst 66(6): 439-446.

16. Kutnar, A., Kamke, F.A., Sernek, M., 2009: Density profile and morphology of viscoelastic thermal compressed wood. Wood Science and Technology 43(1): 57-68.

17. Kutnar, A., Humar, M., Kamke, F.A., Sernek, M., 2011: Fungal decay of viscoelastic thermal compressed (VTC) wood. European Journal of Wood and Wood Products 69(2): 325-328.

18. Laine, K., Segerholm, K., Wålinder, M., Rautkari, L., Hughes, M., 2016: Wood densification and thermal modification: hardness, set-recovery and micromorphology. Wood Science and Technology 50(5): 883-894.

19. Li, M, 2017: Evaluating rolling shear strength properties of cross-laminated timber by short-span bending tests and modified planar shear tests. Journal of Wood Science 63(4): 331-337.

20. Neyses, B., 2016: Surface-densified wood. Licentiate thesis. Department of Engineering Sciences and Mathematics. Luleå: Luleå University of Technology. Pp 14 – 15.

21. Pelit, H., Sönmez, A., Budakçı, M., 2014: Effects of ThermoWood® process combined with thermo-mechanical densification on some physical properties of Scots pine (*Pinus sylvestris L.*). BioResources 9(3): 4552-4567.

22. Pelit, H., Budakçi, M., Sönmez, A., 2016: Effects of heat post-treatment on dimensional stability and water absorption behaviours of mechanically densified Uludağ Fir and Black poplar woods. BioResources 11(2): 3215-3229.

23. Pelit, H., Budakçı, M., Sönmez, A., 2018: Density and some mechanical properties of densified and heat post-treated Uludağ fir, linden and black poplar woods. European Journal of Wood and Wood Product 76(1): 79–87.

24. Pelit, H., Yorulmaz, R., 2019: Influence of densification on mechanical properties of thermally pretreated spruce and poplar wood. BioResources 14(4): 9739-9754.

_____

25. Rautkari, L., Kamke, F.A., Hughes, M., 2011: Density profile relation to hardness of viscoelastic thermal compressed (VTC) wood composite. Wood Science and Technology 45(4): 693-705.

26. Serrano, E., Enquist, B., 2010: Compression strength perpendicular to grain in cross-laminated timber (CLT). 11th World Conference on Timber Engineering (WCTE 2010). Riva del Garda, Trentino, Italy.

27. Shi, J., Peng, J., Huang, Q., Cai, L., Shi, S.Q., 2020: Fabrication of densified wood via synergy of chemical pretreatment, hot-pressing and post mechanical fixation. Journal of Wood Science 66(1): 1-9.

28. Sikora, K.S., McPolin, D.O., Harte, A.M., 2016: Effects of the thickness of cross-laminated timber (CLT) panels made from Irish Sitka spruce on mechanical performance in bending and shear. Construction and Building Materials 116: 141-150.

29. Tan Y.F., Liew, K.C., 2021: Morphological and bending properties of lab-scaled prototype Cross-laminated timber manufactured with densified layered composite from fast-growing tree. Manuscript submitted for IOP Conference Series: Earth and Environmental Science Publication.

30. Tu, D., Su, X., Zhang, T., Fan, W., Zhou, Q., 2014: Thermo-mechanical densification of *Populus tomentosa* var. tomentosa with low moisture content. BioResources 9(3): 3846-3856.

31. Wagner, L., Bader, T.K., Ters, T., Fackler, K., Borst, K.D., 2015: A combined view on composition, molecular structure, and micromechanics of fungal degraded softwood. Holzforschung 69(4): 471–482.

KANG CHIANG LIEW*, YU FENG TAN
UNIVERSITI MALAYSIA SABAH
FACULTY OF TROPICAL FORESTRY
JALAN UMS, 88400 KOTA KINABALU
SABAH
MALAYSIA
*Corresponding author: liewkc@ums.edu.my